Received: 9 September 2022 | Revised: 24 February 2023 | Accepted: 25 February 2023

DOI: 10.1002/rcm.9499

RESEARCH ARTICLE

Rapid Communications in Mass Spectrometry WILEY

Equilibrium isotope fractionation factors of H exchange between steam and soil clay fractions

Stefan Merseburger[1] | Arnim Kessler[2] | Yvonne Oelmann[2] | Wolfgang Wilcke[1]

[1]Institute of Geography and Geoecology, Karlsruhe Institute of Technology (KIT), Karlsruhe, Germany

[2]Geoecology, University of Tübingen, Tübingen, Germany

Correspondence
W. Wilcke, Institute of Geography and Geoecology, Karlsruhe Institute of Technology (KIT), Reinhard-Baumeister-Platz 1, 76131 Karlsruhe, Germany.
Email: wolfgang.wilcke@kit.edu

Funding information
Deutsche Forschungsgemeinschaft, Grant/Award Number: WI1601/25-1

Rationale: Steam equilibration overcomes the problem of the traditional measurements of H isotope compositions, which leave an arbitrary amount of adsorbed water in the sample, by controlling for the entire exchangeable H pool, including adsorbed water and hydroxyl-H. However, the use of steam equilibration to determine nonexchangeable stable H isotope compositions in environmental media (expressed as δ^2H_n values) by mathematically eliminating the influence of exchangeable H after sample equilibration with waters of known H-isotopic composition requires the knowledge of the equilibrium isotope fractionation factor between steam-H and exchangeable H of the sample ($\alpha_{ex\text{-}w}$), which is frequently unknown.

Methods: We developed a new method to determine the $\alpha_{ex\text{-}w}$ values for clay minerals, topsoil clay fractions, and mica by manipulating the contributions of exchangeable H to the total H pool via different degrees of post-equilibration sample drying. We measured the δ^2H values of steam-equilibrated mineral and soil samples using elemental analyzer-pyrolysis-isotope ratio mass spectrometry.

Results: The $\alpha_{ex\text{-}w}$ values of seven clay minerals ranged from 1.071 to 1.140, and those of 19 topsoil clay fractions ranged from 0.885 to 1.216. The $\alpha_{ex\text{-}w}$ value of USGS57 biotite, USGS58 muscovite, and of cellulose was 0.965, 0.871, and 1.175, respectively. The method did not work for kaolinite, because its small exchangeable H pool did not respond to the selected drying conditions. Structurally different mineral groups such as two- and three-layer clay minerals or mica showed systematically different $\alpha_{ex\text{-}w}$ values. The $\alpha_{ex\text{-}w}$ value of the topsoil clay fractions correlated with the soil clay content ($r = 0.63$, $P = 0.004$), the local mean annual temperature ($r = 0.68$, $P = 0.001$), and the δ^2H values of local precipitation ($r = 0.72$, $P < 0.001$), likely to reflect the different clay mineralogy under different weathering regimes.

Conclusions: Our new $\alpha_{ex\text{-}w}$ determination method yielded realistic results in line with the few previously published values for cellulose. The determined $\alpha_{ex\text{-}w}$ values were similar to the widely assumed values of 1.00–1.08 in the literature, suggesting that the adoption of one of these values in steam equilibration approaches is appropriate.

1 | INTRODUCTION

Stable hydrogen isotope compositions (expressed as δ^2H values relative to the standard mean ocean water) are widely used to investigate the provenance of organic substances like collagen, keratin, cellulose, or microbial tissue.[1] When complex materials like soil and plant samples are studied, the measurement of the δ^2H values can be influenced by unwanted exchange of part of the H pool, termed "exchangeable," with ambient atmospheric water vapor during sample preparation, for example. The latter does not affect the "nonexchangeable" part of the H pool stored as C-bonded H in organic matter or structural H in hydroxyl groups. However, the quickly exchanging H can blur the stable H isotope signal of the nonexchangeable H pool.[2–5] Steam equilibration avoids this problem by controlling the influence of the exchangeable H on the δ^2H values of the nonexchangeable H pool. The latter is reached by equilibrating the H isotope composition of exchangeable H with water vapors of known H-isotopic composition. After steam equilibration, the contribution of exchangeable to total H (χ_e) and the nonexchangeable H isotope ratios (δ^2H_n) can be determined by a regression of the measured δ^2H values (δ^2H_t) in equilibrated samples on the known δ^2H values of equilibration water vapors (δ^2H_w; Equation [1]):

$$\delta^2H_t = \chi_e\alpha_{ex-w}\delta^2H_w + (1-\chi_e)\delta^2H_n + 1000\chi_e(\alpha_{ex-w}-1). \quad (1)$$

From this empirical regression line, χ_e (included in the slope) and the δ^2H_n value (included in the *y*-axis intercept) can be calculated if the equilibrium fractionation factor between exchangeable H of the sample and equilibration water ($\alpha_{ex\text{-}w}$) is known. $\alpha_{ex\text{-}w}$ is defined as the ratio of the stable isotope ratio of the exchangeable H in the samples to the stable H isotope ratio of the steam. To the best of our knowledge, there is no established method to determine $\alpha_{ex\text{-}w}$ values for complex mixtures of compounds commonly occurring in soils in the temperature range used for steam equilibration at 110°C –130°C. Schimmelmann[6] determined the $\alpha_{ex\text{-}w}$ value of cellulose by steam equilibration of fibrous cellulose and its nitrated counterpart using a reduced exchangeable H concentration at 114°C for 20 h. From the intersection of the two resulting regression lines for the original cellulose and the nitrated cellulose, Schimmelmann[6] calculated an $\alpha_{ex\text{-}w}$ value of 1.08. This $\alpha_{ex\text{-}w}$ value has been widely used to determine δ^2H_n values of various organic compounds, plants, soil organic matter, and bulk soil by steam equilibration,[7–15] although it is known that the $\alpha_{ex\text{-}w}$ values of cellulose can range from 1.063 to 1.243 depending on its crystallinity.[16–19] Other studies that applied a steam equilibration method to organic materials and clay minerals ignored equilibrium fractionation between exchangeable H in the studied material and ambient water vapor-H, thus assuming an $\alpha_{ex\text{-}w}$ value of 1.[17,20–23]

Recently, Merseburger et al[23] adapted and tested the steam equilibration method of Ruppenthal et al[9] for clay minerals and soil clay fractions. In the hygroscopic clay minerals, in which not only adsorbed water contributes to the exchangeable H pool but also hydroxyl-H at the mineral edges, which cannot be removed by drying,[2] there is a particular risk of exchanging H with ambient atmospheric water vapor after steam equilibration, which needs to be avoided.[2–5] The latter can be reached by closing the samples in airtight tin capsules under an Ar atmosphere, which require less mechanical force for crimping than Ag capsules.[23–25] For samples with a high χ_e value, the calculated δ^2H_n values respond sensitively to variations in the $\alpha_{ex\text{-}w}$ value, because the $\alpha_{ex\text{-}w}$ value influences both the slope and the intercept of the regression line of δ^2H_t values of the studied sample on the δ^2H_w values used for the exchange (Equation [1]).[8,13,19,22,26] Thus, the knowledge of a sample-specific $\alpha_{ex\text{-}w}$ value might improve the measurement of δ^2H_n, particularly if the sample consists of an unknown mixture of different minerals.

The fact that the χ_e value influences the slope of the regression line of measured δ^2H_t values on the known δ^2H_w values provides the opportunity to determine the $\alpha_{ex\text{-}w}$ value by manipulating χ_e, provided that the $\alpha_{ex\text{-}w}$ values remain unchanged. Because part of the exchangeable H pool consists of adsorbed water, different sample drying conditions result in different χ_e values. Analogous to the approach of Schimmelmann,[6] from the intersection point of the pair of regression lines with different slopes resulting from two different drying conditions, $\alpha_{ex\text{-}w}$ can be calculated, provided the difference in the slopes is sufficiently large to precisely determine the intersection point.[6]

In a previous work, Merseburger et al[23] tested whether the classic clay separation treatment, including the removal of Fe oxides and carbonates, reduction of soil organic matter (SOM), and dispersion of the remaining material, affects the δ^2H_n values of clay minerals. In the absence of a known $\alpha_{ex\text{-}w}$ value, the equilibrium fractionation between the exchangeable H pool and the steam-H was ignored (i.e., $\alpha_{ex\text{-}w} = 1$). Merseburger et al[23] found that the differences in δ^2H_n values between clay minerals (kaolinite, illite, montmorillonite, and vermiculite) subjected and not subjected to the clay separation treatment were not significant and concluded that the clay separation treatment did not affect the δ^2H_n values of clay minerals and soil clay fractions. However, this conclusion can be maintained only if the clay separation treatment did not change $\alpha_{ex\text{-}w}$, which remains to be tested.

Ruppenthal et al[8] reported a correlation between the modeled δ^2H values of local mean annual precipitation and the δ^2H_n values of a global set of bulk soil samples. A study of an Argentinian climosequence demonstrated a weaker correlation of the δ^2H values of local precipitation with the δ^2H_n values of bulk soil than with the δ^2H_n values of demineralized SOM.[10,27] Merseburger et al[24] showed that one reason for the weaker correlation of the δ^2H values of local precipitation with the δ^2H_n values of bulk soil than of SOM is the weaker correlation of the δ^2H values of local precipitation with the δ^2H_n values of clay fractions than of SOM assuming the same constant $\alpha_{ex\text{-}w}$ values for all samples. The larger scatter in the relationship between the δ^2H_n values of soil clay fractions and the δ^2H values of local precipitation was attributed to different isotope fractionation between ambient water-H and H of clay minerals ($\alpha_{min\text{-}water}$) during their formation[28] and a minor contribution of rock-derived clay minerals that were not formed under the current climatic conditions. It is, however, additionally possible that this larger scatter

compared to the work of Ruppenthal et al[8,10,27] is also attributable to a potential difference in the $\alpha_{ex\text{-}w}$ values, which might reflect the types of clay minerals. Different types of clay minerals (a) tend to form under different weathering regimes.[29–32] (b) Savin and Epstein[28] found different $\alpha_{min\text{-}water}$ values for kaolinite typically formed under strong chemical weathering conditions (0.97) and montmorillonite more characteristic of moderate weathering (0.94), and it seems possible that similar differences exist for $\alpha_{ex\text{-}w}$. Furthermore, (c) for glauconite, chlorite, mica, and montmorillonite the $\alpha_{min\text{-}water}$ values varied with the octahedral Fe concentration,[33–35] and the chemical composition of clay minerals and soil clay fractions could also influence $\alpha_{ex\text{-}w}$. In addition, the Fe oxide concentration in soil is strongly linked to the weathering regime, with Fe oxides being an important component of soil clay fractions,[30,36] and the octahedral Fe concentrations might be related with the Fe oxide concentrations. Moreover, (d) the different crystal structures and imperfect lattices can influence the availability of hydroxyl groups for H exchange.[11,18,35,37–39] For instance, kaolinite has one quarter of the hydroxyl groups in the same layer as the non-bridging oxygen atoms of the tetrahedral sheet, which are less accessible than the rest of hydroxyl groups on the surface of the microcrystals, which show different vibrational energies and different H exchange rates.[35,39,40] As a consequence, Méheut et al[41] calculated different equilibrium fractionation factors with water for both hydroxyl types of kaolinite.

Our aims were (a) to determine sample-specific $\alpha_{ex\text{-}w}$ values for individual clay minerals and soil clay fractions by manipulating the contribution of exchangeable to total H (χ_e) via differently intensive drying assuming that this does not change the $\alpha_{ex\text{-}w}$ values and (b) to test whether the conventional method to collect soil clay fractions influences $\alpha_{ex\text{-}w}$. Moreover, (c) we tested the hypothesis that the $\alpha_{ex\text{-}w}$ values of soil clay fractions are influenced by their mineralogical composition as assessed via the potential cation-exchange capacity (CEC_{pot}) and their latitudinal and elevational position assessed via the δ^2H value of the local precipitation at the sampling location.

2 | MATERIALS AND METHODS

2.1 | Samples

We used kaolinite (KGa-2), dioctahedral illite (IMt-2), Na-saturated montmorillonite (SWy-3), and Mg-rich trioctahedral montmorillonite (SCa-3) provided by the Clay Mineral Society (Chantilly, VA, USA) and a trioctahedral vermiculite (contributed by Stefan Dultz, Hannover, Germany) as clay mineral reference materials. SCa-3 and IMt-2 were delivered as brittle rock chips, with a macroscopically visible heterogeneity in grain sizes and colors. SWy-3 and KGa-2 were delivered as fine-grained powders. The standards are described by the baseline studies of the Clay Minerals Society Source Clays[42–48] and by Hower and Mowatt[49] for IMt-2. Trioctahedral vermiculite was characterized by Dultz et al,[50] Bors et al,[51] and Steudel et al.[52,53] Furthermore, we included USGS57 biotite and USGS58 muscovite described by Qi et al[54] and microcrystalline cellulose (A17730 Alfa Aesar, Ward Hill, MA, USA).

We used 22 topsoil samples from nine countries on five continents (Table 1; Table S1 [supporting information]). Nine samples originated from a climosequence in Argentina (signature "AR"), which are described in detail in Ruppenthal et al.[10] The Argentinian samples were collected from the 0–10 cm mineral soil layer of Phaeozems (AR-2A and AR-4A), a Chernozem (AR-5C), a Calcisol (AR-14A), a Solonetz (AR-16A), a Luvisol (AR-17A), a Vertisol (AR-19A), and a Planosol (AR-20C). The clay contents ranged from 10% to 30% and organic C concentrations from 5 to 14 g kg^{-1}. The sample DE-KA1 originated from the 7–13 cm depth layer of a Gleysol near Karlsruhe, Germany, with a clay content of 58% and an organic C concentration of 55 g kg^{-1}.[23] The signature "EC" refers to samples from tropical forest sites in south Ecuador.[55,56,58] EC-BOM was collected from the 0–25 cm layer of a Cambisol at an elevation of∼3000 m above sea level and EC-SF from the 0–15 cm layer of a Cambisol at an elevation of ∼2000 m above sea level. The clay contents were 29% and 22%, and the organic C concentrations were 24 and 22 g kg^{-1}. The sample KE-44 originated from the 0–10 cm layer of a Cambisol in Kenya, had a clay content of 71% and an organic C concentration of 48 g kg^{-1}, and was provided by Sadadi Ojoatre.[59] Sample PA-A9 originated from the 0–10 cm layer of a Luvisol on Barro Colorado Island, Panama, and had a clay content of 84% and an organic C concentration of 28 g kg^{-1}.[60,61] The signature "RU" refers to Russia. Sample RU-17 was collected from the 0–30 cm layer of a Luvisol, RU-PS2 from the 0–8 cm layer of a Cryosol, and RU-S20 from the 0–10 cm layer of a Luvisol. The Russian samples had a clay content of 4%–13% and an organic C concentration of 20–78 g kg^{-1}.[62–64] Sample SK-Oso originated from the 0–10 cm layer of a Cambisol in Slovakia and had a clay content of 15% and an organic C concentration of 60 g kg^{-1}.[65,66] Finally, UZ-K1 originated from the 0–10 cm layer of a Calcisol in Uzbekistan with a clay content of 30% and an organic C concentration of 14 g kg^{-1}.[67,68] All samples were dried and stored in the dark for 1–28 years. Further properties of the used soil samples, including X-ray powder diffractometric patterns of six samples, can be found in Merseburger et al.[24] Additional X-ray powder diffractometric patterns have been published for sample PA-A9[60] and from soils nearby the locations from where our three Ecuadorian samples were collected.[57]

2.2 | Clay separation

We used the clay separation method of Merseburger et al,[23] which was thoroughly tested and found to not affect the δ^2H_n values of clay minerals typically occurring in soils. In contrast, the clay separation method, of course, influences the δ^2H values of the exchangeable H pool. This is, however, not relevant for our measurement of δ^2H values, because we anyway equilibrate all exchangeable H with water vapors of known H-isotopic composition in our steam equilibration method (Equation [1]). Briefly, after sieving to <2 mm we removed Fe

TABLE 1 Results of steam equilibration with weaker ("w"), medium ("m"), and stronger ("s") drying intensities (see Figure 1), including the equilibrium fractionation factor between the exchangeable H pool of the sample and the H of the steam ($\alpha_{ex\text{-}w}$), the contribution of exchangeable H to total H (χ_e) after weaker and stronger drying, the δ^2H_n values calculated using sample-specific $\alpha_{ex\text{-}w}$ value and for $\alpha_{ex\text{-}w} = 1$, and the potential cation-exchange capacity (CEC_{pot}).

Type	Sample [reference]	Treatment	Equilibration line pairs	$\alpha_{ex\text{-}w}$ [a]	$\chi_{e,\ weaker}$ [b] (%)	$\chi_{e,\ stronger}$ [b] (%)	δ^2H_n [b] (‰)	$\delta^2H_{n,\ \alpha=1}$ [b] (‰)	CEC_{pot} ($mmol_c\ kg^{-1}$)
Clay mineral	IMt-2 illite[c]	Treated	ws	1.079	13	8	−141	nd	nd
		Untreated	wm, ws	1.134 ± 0.005	21 ± 2	14 ± 1	−158 ± 4	−138 ± 4	89
	SCa-3 montmorillonite[c]	Treated	ws	1.140	38	22	−160	nd	nd
		Untreated	wm, ws, ms	1.084 ± 0.015	75 ± 5	54 ± 4	−202 ± 15	−98 ± 17	1,113
	SWy-3 montmorillonite[c]	Treated	ws	1.122	16	10	−150	nd	nd
		Untreated	wm, ws	1.071 ± 0.032	31 ± 3	22 ± 2	−150 ± 7	−133 ± 7	743
	Trioctahedral vermiculite[c,d]	Untreated	ws, ms	1.090 ± 0.039	71 ± 6	54 ± 3	−225 ± 13	−95 ± 13	nd
Other	USGS57 biotite[54]	Untreated	wm, ws	0.965 ± 0.019	7 ± 1	4 ± 1	−94 ± 1	−95 ± 1	nd
	Microcrystalline cellulose		ws	1.175	25	21	−51	nd	nd
	USGS58 muscovite[54]		wm	0.871	3	2	−29	−31 ± 1	nd
Topsoil clay fraction	AR-2A[10]	Treated	ws, ms	1.129 ± 0.030	45 ± 3	31 ± 3	−162 ± 9	−91 ± 10	261
	AR-4A[10]		wm, ws, ms	1.060 ± 0.027	57 ± 4	40 ± 3	−158 ± 8	−108 ± 8	199
	AR-5C[10]		ws, ms	1.099 ± 0.077	41 ± 4	31 ± 3	−168 ± 8	−118 ± 5	217
	AR-10A[10]		wm, ws, ms	1.100 ± 0.006	49 ± 3	28 ± 2	−157 ± 2	−106 ± 2	531
	AR-14A[10]		wm, ws, ms	1.070 ± 0.019	53 ± 4	30 ± 4	−156 ± 8	−118 ± 8	248
	AR-16A[10]		wm, ws, ms	1.087 ± 0.046	51 ± 5	33 ± 5	−176 ± 7	−129 ± 5	497
	AR-17A[10]		wm, ws, ms	1.091 ± 0.042	49 ± 4	32 ± 3	−180 ± 9	−129 ± 8	664
	AR-19A[10]		wm, ws, ms	1.080 ± 0.000	45 ± 2	26 ± 3	−168 ± 2	−132 ± 2	640
	AR-20C[10]		wm, ws, ms	1.080 ± 0.052	54 ± 6	36 ± 4	−191 ± 10	−132 ± 5	423
	DE-KA1[23]		wm, ws	1.129 ± 0.023	37 ± 2	28 ± 2	−146 ± 6	−94 ± 7	296
	EC-BOM[55–57]		wm	1.114	31	30	−101	−61 ± 2	127
	EC-SF1[55,57,58]		wm	0.979	19	16	−67	−71 ± 2	143
	KE-44[59]		ws	1.216	41	32	−168	−56 ± 2	344
	PA-A9[60,61]		wm, ws	1.150 ± 0.035	35 ± 2	22 ± 2	−129 ± 5	−85 ± 5	872
	RU-17[62,63]		wm, ws	1.094 ± 0.011	39 ± 3	26 ± 2	−138 ± 6	−101 ± 6	241
	RU-PS2[64]		ws, ms	0.885 ± 0.105	26 ± 5	20 ± 4	−140 ± 8	−167 ± 1	240
	RU-S20[62,63]		wm, ws, ms	1.007 ± 0.036	40 ± 3	26 ± 2	−139 ± 4	−136 ± 2	114

TABLE 1 (Continued)

Type	Sample [reference]	Treatment	Equilibration line pairs	$\alpha_{ex\text{-}w}$ [a]	$\chi_{e,\ weaker}$ [b] (%)	$\chi_{e,\ stronger}$ [b] (%)	δ^2H_n [b] (‰)	$\delta^2H_{n,\ \alpha=1}$ [b] (‰)	CEC_{pot} ($mmol_c\ kg^{-1}$)
	SK-Oso[65,66]		wm, ws, ms	1.024 ± 0.024	21 ± 1	16 ± 1	−105 ± 3	−99 ± 3[e]	121
	UZ-K1[67,68]		wm, ws	1.205 ± 0.011	26 ± 1	17 ± 2	−148 ± 6	−102 ± 6	311

Notes: The δ^2H_n values for $\alpha_{ex\text{-}w} = 1$ and the CEC_{pot} were taken from previous studies.[23,24] "Untreated" and "treated" indicate samples not subjected and subjected to clay separation, including removal of Fe oxides and carbonates, reduction in SOM, and dispersion of the remaining material.
Abbreviations: nd, not determined; SOM, soil organic matter.
[a]Mean ± standard error calculated from $\alpha_{ex\text{-}w}$ determinations using two or three pairs of regression lines of the δ^2H value of the sample on the δ^2H value of the waters used for steam equilibration.
[b]With standard deviation, derived by Gaussian error propagation (Text S2).
[c]Reference is given in the text, Section 2.1.
[d]The result of the treated trioctahedral vermiculite showed an inacceptable standard deviation above 0.2 and was therefore omitted.
[e]Mean and standard deviation of δ^2H_n from four independent measurements.

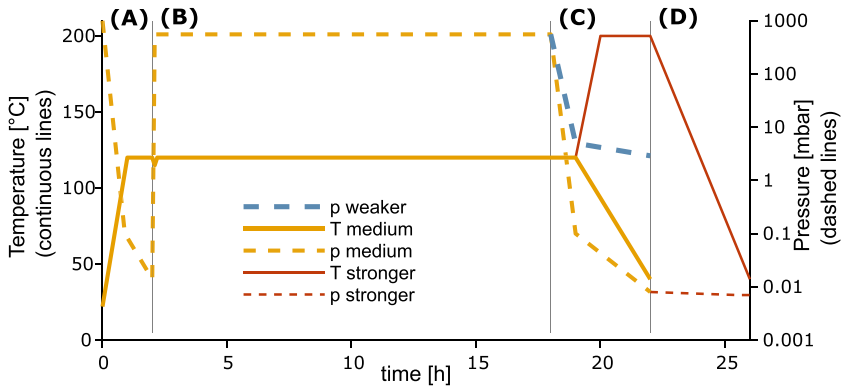

FIGURE 1 Temperature and pressure conditions during equilibration of soil clay fractions and clay minerals with water vapor of known H-isotopic composition. A, the drying phase before equilibration; B, the equilibration phase; C and D, two stages of the drying phase. The continuous yellow line shows the standard procedure (medium drying). If deviating from the standard procedure, temperature (continuous lines) and pressure (dashed lines) are plotted for stronger drying (red, thin lines) and for weaker drying (blue, thick, dashed line), for which only the pressure was less decreased. [Color figure can be viewed at wileyonlinelibrary.com]

oxides by applying the dithionite-citrate-buffer method of Mehra and Jackson[69] once. To remove carbonates, we used a Na–acetate acetic acid buffer adjusted to pH 4.8. To remove organic matter, we added H_2O_2 in a water bath at 50°C. We removed water-soluble salts with several washing cycles using water or salt solutions after each mineral or SOM destruction step. After the electrical conductivity of the supernatants of the sample solution had reached <400 µS cm^{-1}, we determined the grain sizes by pipette analysis according to DIN ISO 11277,[70] but instead of a dispersion agent we used water with a pH of ~7.5. In this water, we separated the grain sizes by repeated sedimentation in 2-L cylinders. Clay separates were precipitated using $MgCl_2$. A H_2O_2 treatment of the precipitate reduced the organic matter concentration in the clay fractions further. After final washings until the conductivity of the supernatant had reached <100 µS cm^{-1}, we dried the clay fractions at 60°C and pulverized them manually in a mortar.

All samples were distributed among four treatment batches each taking ~10–12 weeks. As quality check, we included sample SK-Oso in each treatment batch, which resulted in relative standard deviations (SD) of 2% for each of the sand, silt, and clay fractions. In a previous study,[23] we found that the differences between clay minerals (kaolinite, illite, montmorillonite, vermiculite) that were subjected ("treated") and not subjected to the clay separation procedure ("untreated") were not significant and concluded that the clay separation treatment did not affect the δ^2H_n values of clay minerals and soil clay fractions.

2.3 | Steam equilibration

We steam equilibrated all samples, which included the soil clay fractions and the pure minerals that were both subjected to the clay separation procedure ("treated") and measured directly ("untreated"). We weighed 1–2 mg of the air-dry and homogeneous sample (2–3.5 mg for USGS biotite and muscovite) in triplicates and transferred into smooth-walled tin capsules of known weight. The samples were vacuum dried for 2 h at 120°C. Then, we injected water of known isotopic composition into the closed stainless-steel vessel. We steam-equilibrated our samples with three to four different waters of known isotopic composition per batch (AWI-TD1: −266.4 ± SD 0.8‰, n = 4; laboratory water: −57.5 ± 0.8‰, n = 3; medium deuterium-enriched water: 136.8 ± 0.6‰, n = 3; and highly deuterium-enriched water: 334.6 ± 1.8‰, n = 4). Within 16 h at the same temperature, the steam-H equilibrated with the exchangeable H fraction of the samples. This was followed by 15 min of vacuum drying using a diaphragm pump (VP 220, VWR, Radnor, PA, USA) and 45 min using a rotary vane pump (RZ 2.5, Vacuubrand, Wertheim, Germany), both at 120°C and a 2 h cooling phase at room temperature under continuous evacuation (≤1 Pa), which we called "medium"-drying intensity. We transferred the vacuum chamber into a glove bag, self-made from 100 µm polyethylene foil bags,[71] and flushed twice with dried Ar to reach a water vapor–free atmosphere. In the Ar atmosphere, we sealed each of the approximately 80 capsules in the vacuum vessel with a gastight pressing. After cooling, each capsule was weighed.

In addition to medium drying, we realized a weaker and a stronger drying intensity. For the weaker drying intensity, the temperature was maintained at 120°C after the 16 h equilibration, and the stainless-steel vessel was evacuated using the diaphragm pump for 1 h. Then, the vessel was cooled for 2 h at room temperature outside the oven while evacuating with the diaphragm pump to a final pressure of 150–300 Pa. For the stronger drying intensity, the temperature was maintained at 120°C after the 16-h equilibration, and the stainless-steel vessel was evacuated using the diaphragm pump for 15 min and additionally with the rotary vane pump for another 45 min. Then, the temperature was increased to 200°C for 2 h, cooled for 3 h at room temperature outside the oven, and evacuated continuously using the rotary vane pump to a final vacuum <1 Pa (Figure 1). To test additionally whether there was an effect of remoistening of the samples after the different drying procedures on their δ^2H_t values, we included SCa-3 montmorillonite (as provided by the Clay Mineral Society but gently ground to <200 µm by hand) considered as particularly hygroscopic in each equilibration batch. We sealed the tin capsules with SCa-3 montmorillonite in triplicate before all other samples in the equilibration batch and again at the end, also in triplicate. We found only a small difference of 2.2 ± SD 2.0‰ between the mean of the triplicate samples sealed at the beginning and the mean of the triplicate samples sealed at the end because of slight remoistening during which we sealed the tin capsules of all samples.

Our different drying intensities reflect conditions used in previous studies in which steam equilibration was applied. For example, the final pressure of our weaker drying intensity is close to the 100 Pa used by Ruppenthal et al[8] and the <500 Pa recommended by Wassenaar et al.[72] The stronger drying intensity at 200°C is by ±50°C similar to the vacuum-drying temperatures used for durations of 2–4 h before conventional δ^2H measurements of clays. Studies investigating the optimum temperature for vacuum drying found that 200°C removes most of the adsorbed water, although some water residues remain depending on the clay mineral type and the degree of crystallinity.[2,5,37,40] Our approach is based on the assumption that the variation in drying procedures did not affect the $\alpha_{ex\text{-}w}$ values. It is reported that the pressure sensitivity of the equilibrium fractionation factor is negligible below 130°C[41,73] and likely still small up to our maximum temperature of 200°C. However, there are two possible problems with this assumption. (a) With the variation in the temperature between 120°C and 200°C, we might slightly change the $\alpha_{ex\text{-}w}$ value, which is an equilibrium constant that is related with temperature. For pure water, the difference in $\alpha_{liquid\text{-}vapor}$ between our lowest temperature of 120°C and our highest one of 200°C was reported to be 0.018 at high pressure.[74] Because we studied adsorbed water, which does not similarly freely exchange between the liquid and gaseous phases under a lower pressure, we assume that the variation in the $\alpha_{ex\text{-}w}$ value created by the different drying pressures is <0.018. (b) We removed different amounts of adsorbed water with different drying intensities. If the removed water had a different H isotope composition than the total exchangeable H pool, then the different removed amounts could also have a small influence on our estimate of the $\alpha_{ex\text{-}w}$ value of the remaining exchangeable H. The latter we have not checked, because this would require to determine specific $\alpha_{ex\text{-}w}$ values for different fractions of exchangeable H, which was beyond our time and money resources.

2.4 | Hydrogen isotope ratio measurement

We used the H isotope ratio measurement, clay separation, and steam equilibration methods of Merseburger et al.[23,24] Briefly, after weighing the cooled capsules, we measured the δ^2H values using an elemental analyzer-pyrolysis- isotope ratio mass spectrometer (Flash 2000 HTC−Delta V Advantage, Thermo Fisher, Waltham, MA, USA) in a chromium-filled Al_2O_3 reactor at 1250°C. We corrected small memory effects with the help of a pool-wise memory correction algorithm using one or two pools.[75] For normalization, we used VSMOW (Vienna Standard Mean Ocean Water), SLAP, and IAEA-604 in silver capsule triplicates (25 µl, USGS, Reston, VA, USA) for each measurement sequence.

To control for instrumental drift between October 20, 2020, and May 21, 2021, we measured in each elemental analyzer-pyrolysis-isotope ratio mass spectrometry (EA−IRMS) sequence a polyethylene powder used as in-house standard with a mean δ^2H value of −70.2 ± SD 1.7‰ (n = 264), GISP with −189.3 ± 1.1‰ (n = 46), and IAEA-CH7 with −100.6 ± 1.7‰ (n = 90). The standards were not steam equilibrated. These values were indistinguishable from the certified or recommended values. The sample SK-Oso, for which we

collected the clay fraction four times in separate runs to generate independent replicates and which were steam-equilibrated, had a δ^2H_n value of −99 ± SD 3‰ and a χ_e of 17.8 ± 0.8% ($\alpha_{ex\text{-}w} = 1$, medium-drying intensity).

2.5 | Chemical sample properties

The C concentrations were determined using an elemental analyzer (Flash 2000 HTC, Thermo Fisher, Waltham, MA, USA) and a EuroVector 3000 (EuroVector, Pavia, Italy). The pH value was measured with a glass electrode (SenTix® 81 on pH 3310, WTW, Weilheim, Germany) in a deionized water suspension at a soil to water ratio of 1:2.5 (v/v). The CEC_{pot} of the clay fractions was determined using the Cu(II)-triethylentetramine method,[76,77] in a a phosphate buffer (pH = 7.0) and with 24 h shaking time. To differentiate between nonswellable two-layer clay minerals and chlorite and swellable three-layer clay minerals and illite in soil clay separates, which contain a complex mixture of minerals not only consisting of clay minerals, we used a value of 160 $mmol_c\ kg^{-1}$ below which we assumed a dominance of two-layer clay minerals and/or chlorite and above which one of three-layer clay minerals following international soil classification systems.[78] For pure clay minerals, the threshold value of the CEC_{pot} to distinguish between two- and three-layer clay minerals was 400 $mmol_c\ kg^{-1}$.[79] Previous XRD measurements of a subset of our soil clay fractions confirmed that the CEC_{pot} is suitable to approximately assign the clay fractions of the soil samples to the dominant clay mineral groups.[24,57,60]

2.6 | Data evaluation

We normalized all stable H isotope ratios to the VSMOW-SLAP scale,[80] which we extended with IAEA-604 to 799.9‰, and expressed them in ‰ relative to VSMOW.

We used the R statistical computing environment[81,82] to calculate stable H isotope data and for statistical analysis. To determine reliable δ^2H_n values, we removed samples that came into contact with atmospheric humidity after the equilibration. We detected such samples by (a) visual inspection for holes and (b) the absence of an Ar peak after the H_2 peak in the elemental analyzer chromatogram. Steam equilibrations of the same sample with isotopically different waters need to result in the same contribution of exchangeable H to the total H concentration (same χ_e). Moreover, (c) we removed individual H isotope measurements in which both the H concentration and the residual of the equilibrium line were 0.5 times outside the interquartile range of all other equilibrations of the same sample as outliers. This quality check was performed individually for all capsules subjected to steam equilibration by performing steps (b) and (c) simultaneously in an automated script. We regressed the measured δ^2H_t values on the known isotopic H composition of the equilibration waters (δ^2H_w) and used Equation (1) to determine δ^2H_n values and the contribution of exchangeable to the total H concentration (χ_e).[8–10,13,16,19,26] The intercept (b) of the regression line is a function of χ_e, δ^2H_n, and $\alpha_{ex\text{-}w}$. The slope (m) is the product of χ_e and $\alpha_{ex\text{-}w}$. For $\delta^2H_w = 0$, Equation (1) can be solved for δ^2H_n using each individual regression line (i) originating from a specific drying procedure (Equation [2]):

$$\delta^2H_{n,i} = \frac{\alpha_{ex-w}\, b_i - 1000 m_i\,(\alpha_{ex-w} - 1)}{\alpha_{ex-w} - m_i}. \quad (2)$$

By drying the samples after equilibration differently, the slope (m_i) and intercept (b_i) of the equilibration line can be manipulated because χ_e is varied and as a consequence also the δ^2H_t values.

Assuming that $\alpha_{ex\text{-}w}$ and δ^2H_n values of the different drying procedures are the same and solving Equation (2) for $\alpha_{ex\text{-}w}$ yields Equation (3):

$$\alpha_{ex-w} = \frac{b_1 m_2 - b_2 m_1 + 1000(m_2 - m_1)}{b_1 - b_2 + 1000(m_2 - m_1)}. \quad (3)$$

For confirmation, we calculated $\alpha_{ex\text{-}w}$ using two other methods, with the identical result (Text S1 [supporting information]). We estimated the standard error of $\alpha_{ex\text{-}w}$ by applying Gaussian error propagation (Text S2 [supporting information]). A larger difference between the slopes and a smaller scatter around the equilibration lines resulted in a smaller propagated error. We accepted only $\alpha_{ex\text{-}w}$ values with a propagated SD <0.2. Moreover, we used pairs of equilibration lines only if the stronger drying resulted in a steeper slope than the weaker drying. Including the medium-drying equilibration line taken from Merseburger et al,[23,24] when available, yielded a maximum of three possible equilibration line pairs and thus three opportunities for deriving $\alpha_{ex\text{-}w}$. We then calculated the arithmetic mean and standard error as a measure of the precision of the estimate of the mean of the $\alpha_{ex\text{-}w}$ values from different combinations of equilibration line pairs.

For the sampling locations of the topsoil clay fractions, we considered mean annual precipitation and temperature using the Worldclim (version 2) data set for the years 1970–2000[83] with derived evapotranspiration and aridity index.[84] Annual mean δ^2H values of precipitation (δ^2H_p) were computed using the Online Isotopes in Precipitation Calculator.[85,86]

3 | RESULTS AND DISCUSSION

3.1 | Determination of sample-specific $\alpha_{ex\text{-}w}$ values

In line with the sufficiently different slopes of the regression lines, there was a significant difference between the contributions of exchangeable H to total H (χ_e) in the minerals and clay fractions after weaker and stronger drying (paired t-tests, mean difference: 11.2%, $P < 0.001$), ranging from 1% to 24% (Table 1). Thus, the different drying procedures allowed for the calculation of a sample-specific $\alpha_{ex\text{-}w}$ value.

We were able to determine the $\alpha_{ex\text{-}w}$ value for 7 of 10 clay minerals, 19 of 22 topsoil clay fractions, and all 3 other materials (two different types of mica and cellulose, Table 1). The missing data are attributable to the fact that the slopes of the regression lines of the δ^2H_t values of the sample on the δ^2H_w values after the different drying procedures were not sufficiently different to reliably determine the intersection point of the two regression lines in all three considered pairs (weaker-medium, weaker-stronger, and medium-stronger drying). The overall mean $\alpha_{ex\text{-}w}$ value was 1.080 ± standard error (SE) 0.015 (n = 29) and thus identical with the $\alpha_{ex\text{-}w}$ value frequently chosen in the literature for bulk soil and organic matter.[8] Thus, an $\alpha_{ex\text{-}w}$ value of 1.080 is a suitable estimate for soil minerals.

For USGS57 biotite, only the slopes of the regression lines of the δ^2H_t values of the sample on the δ^2H_w values between weaker drying and medium-stronger drying were sufficiently different, whereas medium and stronger drying resulted in indistinguishable slopes, leaving two of three possible combinations of regression lines for deriving $\alpha_{ex\text{-}w}$ (Figure 2; Table 1). For untreated kaolinite, that is, kaolinite not subjected to clay separation, the regression lines of the three different drying procedures were almost identical, preventing the calculation of an $\alpha_{ex\text{-}w}$ value of this nonswellable two-layer clay mineral (Figure 2). Kaolinite showed a contribution of exchangeable to total H of 7 ± SD 1% and USGS58 muscovite of 1.1 ± 0.6% (for medium drying). In contrast to kaolinite, the $\alpha_{ex\text{-}w}$ determination of the muscovite was possible, because the exchangeable H pool responded to the different drying intensities. This indicated that the exchangeable H pool of the muscovite contained more adsorbed water, whereas that of the kaolinite contained more hydroxyl-H. The swellable two-layer clay minerals, SCa-3 montmorillonite (Figure 2) and trioctahedral vermiculite (Table S1 [supporting information]), strongly responded to the different drying procedures. However, the regression line of the treated trioctahedral vermiculite showed a low coefficient of determination, because of a large scatter around the regression lines (Table S1 [supporting information]), so that the SD of $\alpha_{ex\text{-}w}$ was 0.224 above our proposed threshold for acceptable precision. Consequently, we could not determine a reliable $\alpha_{ex\text{-}w}$ value for treated trioctahedral vermiculite.

The two regression lines after weaker and stronger drying for commercially available cellulose were sufficiently different to determine the $\alpha_{ex\text{-}w}$ value at 1.175 (Figure 2D). This is higher than the

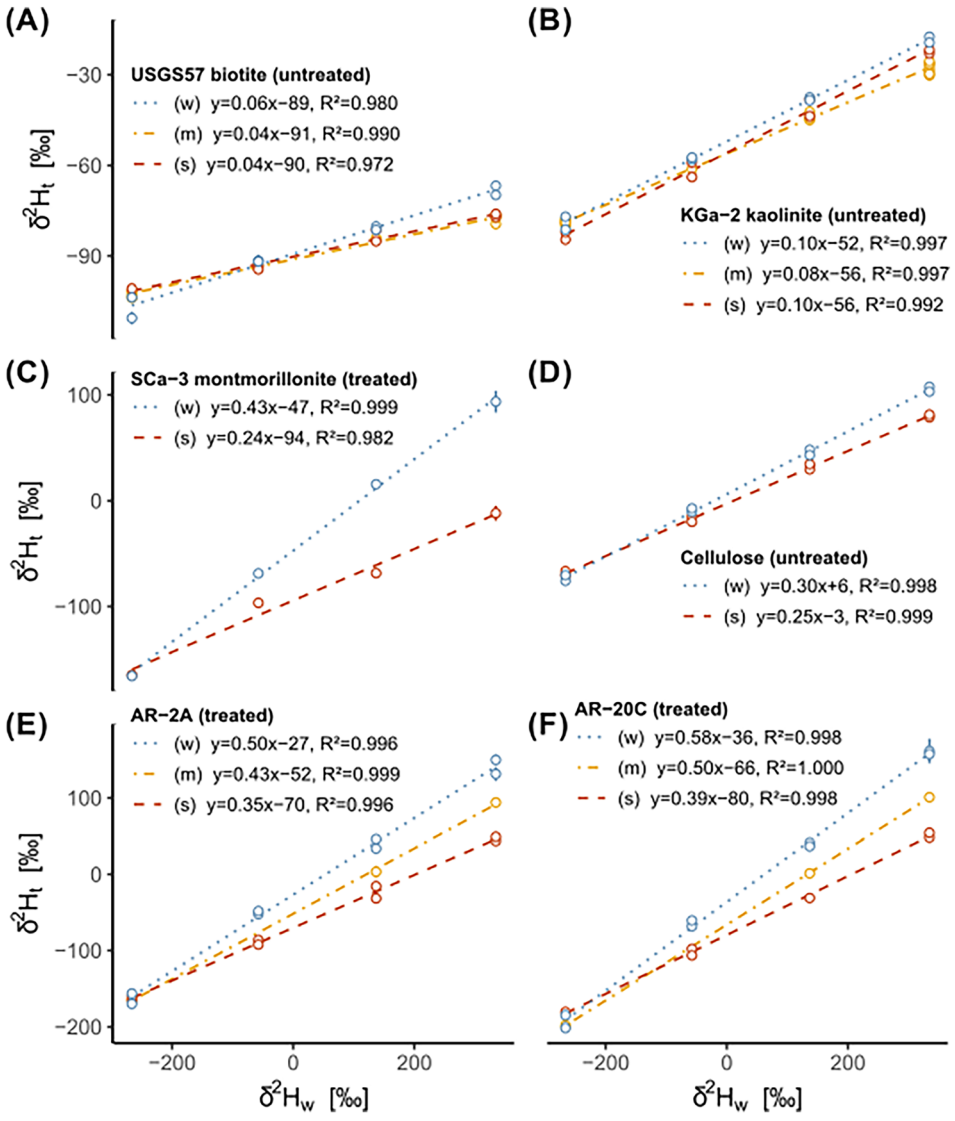

FIGURE 2 Regression lines of the total δ^2H (δ^2H_t) values of A, USGS57 biotite, B, KGa-2 kaolinite, C, SCa-3 montmorillonite, D, cellulose, E, clay fraction of sample AR-2A, and F, clay fraction of sample AR-20C on the δ^2H values of different equilibration waters (δ^2H_w) of selected samples after weaker ("w"), medium ("m"), and stronger ("s") drying. "AR" denotes soil clay fractions from Argentina (Table 1). "Untreated" and "treated" indicate samples not subjected and subjected to clay separation (Section 2.2), respectively. For C, SCa-3 montmorillonite and D, microcrystalline cellulose, no medium-drying intensity was realized. Each point originates from an independent equilibration run, measured in a separate EA–IRMS sequence. Error bars show standard deviations (n = 1–3) and might be smaller than the symbol size. [Color figure can be viewed at wileyonlinelibrary.com]

$\alpha_{ex\text{-}w}$ value of 1.08 determined at 114°C reported by Schimmelmann[6] and of 1.082 determined at 105°C reported by Filot et al,[16] who found a variation in the $\alpha_{ex\text{-}w}$ value for cellulose extracted from different years of tree rings from 1.063 to 1.112. However, our $\alpha_{ex\text{-}w}$ value for cellulose is lower than the reported $\alpha_{ex\text{-}w}$ values of 1.213–1.243 determined at 0°C and 92°C for cellulose extracted from different tree species.[17–19] The differences in the $\alpha_{ex\text{-}w}$ values cannot be explained by the different equilibration temperatures, because there is no obvious relationship between temperature and the $\alpha_{ex\text{-}w}$ value. We therefore speculate that the different reported $\alpha_{ex\text{-}w}$ values of cellulose are related with its crystallinity and thus represent a natural variation. Whereas in the microcrystalline cellulose, which we studied, steam might reach all hydroxyl-H, this is possibly not the case in more crystalline cellulose, where some hydroxyl-H is shielded from steam.[11,18]

For both types of mica (USGS57 biotite and USGS58 muscovite[54]), we found, as the only samples, $\alpha_{ex\text{-}w}$ values <1 (Table 1). We speculate that this might be attributable to the particularly low isoelectric point of pH <2, which is lower than that of many clay minerals, indicating that hydroxyl groups at the mineral edges do not strongly bind protons, which commonly favors the binding of the light H isotope.[87,88]

For most topsoil clay fractions, our different drying procedures resulted in sufficiently different slopes of the regression lines, as illustrated for two soil clay fractions from Argentina in Figures 2E and 2F. For 19 soil clay samples, the mean $\alpha_{ex\text{-}w}$ value was 1.084 ± SE 0.017 (Table 1), which was significantly greater than 1.00 (*t*-test, $P < 0.001$) and thus indicated that there was indeed an equilibrium fractionation between steam-H and the exchangeable H pool. The three topsoil clay fractions for which we could not successfully determine $\alpha_{ex\text{-}w}$ values originated from Thailand and Kenya. The Kenyan samples had high concentrations of dithionite-soluble Fe ranging from 56 to 75 mg g^{-1}. This could be problematic, because octahedral Fe was reported to influence the H isotope fractionation between clay minerals and ambient water during mineral precipitation (i.e., the $\alpha_{min\text{-}water}$ value)[33–35] and by inference might also influence the $\alpha_{ex\text{-}w}$ value. However, this high Fe concentration did not prevent us from determining a meaningful $\alpha_{ex\text{-}w}$ value for the clay fraction of sample KE-44 (Table 1). Moreover, these tropical soil samples possibly contained some kaolinite, for which our approach did not work (Figure 2B). We attribute this to a small exchangeable H pool not responsive to the selected drying conditions in kaolinite and strongly weathered tropical soil samples.

Overall, we found systematic differences in the $\alpha_{ex\text{-}w}$ values of well-defined materials, with the two mica showing the lowest, the three-layer clay minerals intermediate, and cellulose the highest values (Table 1), revealing that these minerals provided different bonding environments for exchangeable H. Because in equilibrium fractionation, the heavy isotopes tend to accumulate in the stronger bonds, a higher $\alpha_{ex\text{-}w}$ value reflects a stronger bonding environment for H.[87] The $\alpha_{ex\text{-}w}$ values of our topsoil clay fractions almost spanned the whole range of $\alpha_{ex\text{-}w}$ values of the well-defined materials reflecting the heterogeneous mineral composition of these samples (Table 1).

3.2 | Influence of clay separation on the $\alpha_{ex\text{-}w}$ values of clay minerals

The differences in the $\alpha_{ex\text{-}w}$ values of the three clay minerals provided by the Clay Mineral Society (IMt-2 illite: 0.055, SCa-3 montmorillionite: −0.056, and SWy-3 montmorillonite: −0.051) between samples not subjected to clay separation ("untreated") and samples subjected to clay separation ("treated") were consistently smaller than the propagated SD of each treated sample (0.099, 0.089, and 0.172, respectively; Table 1; Text S2 [supporting information]). Additionally, a *t*-test for the three pairs of treated and untreated $\alpha_{ex\text{-}w}$ values did not indicate a significant difference ($P = 0.68$). Thus, the clay separation procedure did not change the properties of the studied clay minerals in a way that significantly influenced their $\alpha_{ex\text{-}w}$ values.

For some of the swellable three-layer clay minerals such as trioctahedral vermiculite and SCa-3 montmorillonite, the error of the $\alpha_{ex\text{-}w}$ value determination using our approach was comparatively high and for the treated trioctahedral vermiculite even above the acceptable SD of 0.2 (Table 1). We attribute this to an insufficient control of the final vacuum for weaker drying conditions and still slight remoistening after steam equilibration and drying, because of the particularly high hygroscopicity of these minerals, which should be further reduced in future studies (Text S3 [supporting information]). We quantified the influence of remoistening in the time interval between opening the vacuum vessel in a dried Ar atmosphere and gas-tight sealing of the last capsules using SCa-3-montmorillionite, our most hygroscopic sample (Table 1) in each steam equilibration run. The difference in the δ^2H_t values of SCa-3 montmorillionite between the first and the last capsules averaged 2.2 ± SD 2.0‰. Because of a consistently much flatter slope of the regression lines of the δ^2H_t values of the sample on the δ^2H_w values, we assume this small influence to be negligible for the less hygroscopic soil clay fractions (Table S1 [supporting information]).

For the soil clay fractions, we cannot test the influence of the clay separation as for pure minerals, because the soil clay fractions exist only after this treatment. However, from the lack of an influence of clay separation on the $\alpha_{ex\text{-}w}$ values of several common minerals in soils, we infer that the clay separation did not affect the $\alpha_{ex\text{-}w}$ values of the soil clay fractions.

3.3 | Influence of CEC_{pot} and the δ^2H value of local precipitation on the $\alpha_{ex\text{-}w}$ values of soil clay fractions

The $\alpha_{ex\text{-}w}$ values of the group of soil clay fractions with a $CEC_{pot} \leq 160$ $mmol_c$ kg^{-1}, which was presumably dominated by nonswellable clay minerals with a low surface charge, including two-

layer minerals and pedogenic chlorite,[78] are indicative of a strong weathering environment.[29,32] The group of soil clay fractions with a CEC_{pot} ≤ 160 $mmol_c\ kg^{-1}$ was unrelated with the mean annual δ^2H value of local precipitation (δ^2H_p), which we used as a proxy of the climatic influence at the various latitudinal and elevational locations with decreasing δ^2H_p values from the equator to the pole and from sea level to mountain tops (Figure 3). We attribute this to the small number of four samples, the small variation in δ^2H_p values, and the comparatively large error of the $\alpha_{ex\text{-}w}$ values because of the small χ_e values of these samples.

The $\alpha_{ex\text{-}w}$ values of the group of soil clay fractions with a CEC_{pot} of 160–400 $mmol_c\ kg^{-1}$ presumably containing a mixture of different clay minerals with a higher surface charge, including nonswellable three-layer minerals such as illites and swellable three-layer minerals such as smectites and vermiculite, correlated significantly with the δ^2H_p values. This might reflect an increasing contribution of three-layer clay minerals with increasing latitude and climatically determined decreasing weathering intensity. This is corroborated by the increasing χ_e values with increasing latitude in this group of soil clay fractions (Table 1), because it is known that the χ_e values decrease in the order: swellable three-layer clay minerals > nonswellable three-layer clay minerals (illite) > two-layer clay minerals > mica.[23,24]

The $\alpha_{ex\text{-}w}$ values of the group of soil clay fractions with a CEC_{pot} > 400 $mmol_c\ kg^{-1}$, presumably dominated by swellable three-layer clay minerals, correlated with the δ^2H_p values, but the slope was flatter than that for the group of soil clay fractions with a CEC_{pot} of 160–400 $mmol_c\ kg^{-1}$ (Figure 3). We attribute this finding to the fact that the group of soil clay fractions with a CEC_{pot} > 400 $mmol_c\ kg^{-1}$ contained a less heterogeneous mixture of minerals, possibly dominated by a single three-layer clay mineral.

Our findings are in line with the fact that the hot-humid inner tropical zone at low latitude (and δ^2H_p values near 0) tends to be dominated by two-layer clay minerals, whereas the temperate zone at intermediate latitude and δ^2H_p values shows a prevalence of three-layer clay minerals.[29,31,32] The climatic influence on the $\alpha_{ex\text{-}w}$ values is corroborated by the finding that the $\alpha_{ex\text{-}w}$ values correlated significantly with the clay content of the bulk soil and the mean annual temperature (Figure 4). Intensely weathered tropical soils frequently show higher clay content and a higher mean annual temperature than soils at higher latitude.

Our finding has implications for the interpretation of earlier observations of correlations between δ^2H values of local precipitation and δ^2H values of clay minerals, soil clay fractions, and bulk soils, if the δ^2H values were determined by steam equilibration such as in Merseburger et al[23] and Ruppenthal et al.[8,10,27] The relationship between δ^2H values of local precipitation and δ^2H_n values of clay minerals of the soil clay fraction or bulk soil can, in these cases, be influenced by the varying $\alpha_{ex\text{-}w}$ values of the clay mineral mixture in different soils.

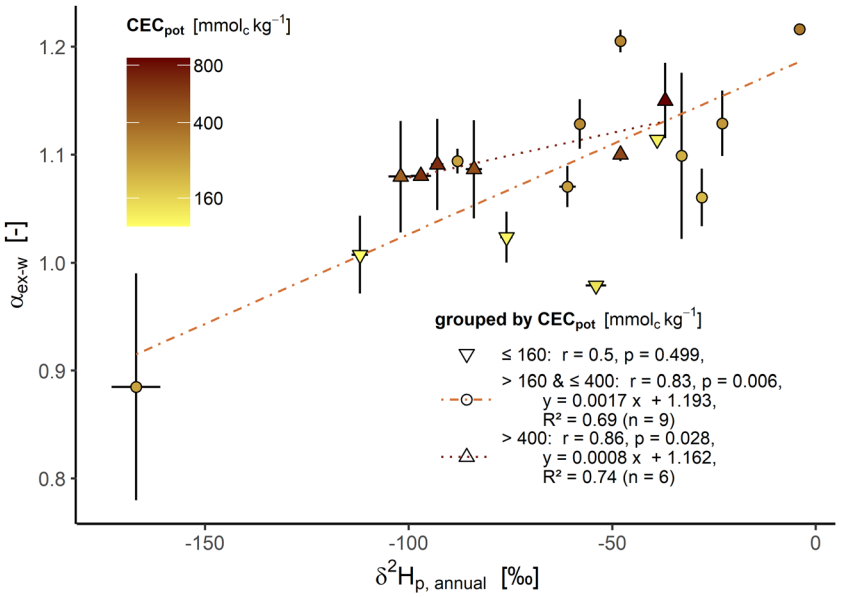

FIGURE 3 Relationship between the δ^2H values of mean annual local precipitation ($\delta^2H_{p,\ annual}$; taken from Bowen[86]) and the specific $\alpha_{ex\text{-}w}$ values of the soil clay fractions. The soil clay fractions are grouped based on the potential cation-exchange capacity (CEC_{pot}) into samples with a CEC_{pot} ≤ 160 $mmol_c\ kg^{-1}$ presumably dominated by nonswellabe clay minerals such as kaolinite and pedogenic chlorite and a CEC_{pot} > 160 to ≤400 $mmol_c\ kg^{-1}$ presumably containing a mixture of different swellable and nonswellable clay minerals such as illite, smectites, and vermiculite, and >400 $mmol_c\ kg^{-1}$ presumably dominated by swellable three-layer clay minerals such as smectites and vermiculite. To illustrate the variation in CEC_{pot} values within these groups, we furthermore color coded the CEC_{pot}. The horizontal error bars indicate the 68% confidence interval and might be smaller than the symbol size. The vertical error bars indicate the standard error (n = 2–3), if available. [Color figure can be viewed at wileyonlinelibrary.com]

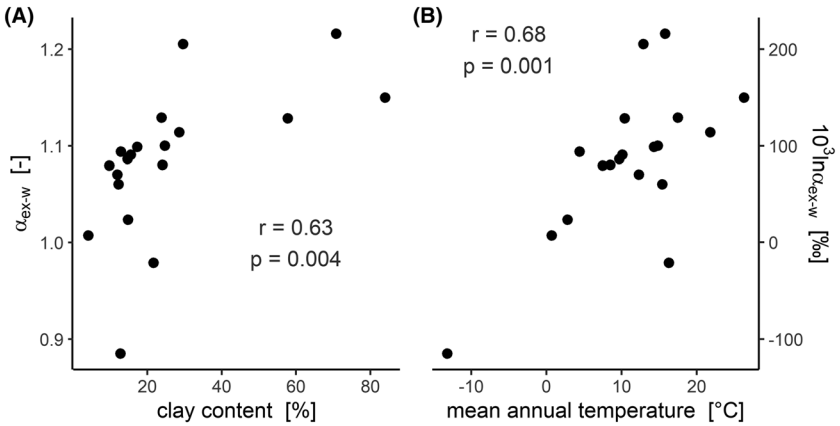

FIGURE 4 Relationship between A, the clay content of bulk soil samples and B, the mean annual temperature at the sampling location and the α_{ex-w} values of the soil clay fractions.

4 | CONCLUSIONS

Steam equilibration with at least two distinctly different drying conditions can be successfully used to determine the equilibrium fractionation factor between the exchangeable H pool of the clay minerals and soil clay fractions and the H of the steam (α_{ex-w}), although partly only with a considerable error. This error, however, includes both the determination error and the heterogeneity in mineralogical composition between aliquots of the same sample and thus also reflects a natural variation. The determined α_{ex-w} values were similar to the widely assumed values of 1.00–1.08 in the literature supporting that the adoption of one of these values in steam equilibration approaches is appropriate. For soil clay fractions and soil clay minerals 1.080 is a suitable average estimate of α_{ex-w}. However, the previously reported correlations between δ^2H values of local precipitation and δ^2H_n values of clay minerals, soil clay fractions, and bulk soils can be influenced by the mineral-specific α_{ex-w} values, if steam equilibration is used to determine the δ^2H_n values.

We did not detect a significant effect of the classical clay separation treatment, including removal of Fe oxides and carbonates, reduction in SOM, and dispersion of the remaining material, on the α_{ex-w} values of clay minerals.

We found that the α_{ex-w} values of topsoil clay fractions are influenced by their mineralogical composition, as assessed via their CEC and latitudinal and elevational locations. The samples with a low CEC tended to show a lower mean α_{ex-w} value than those with a high CEC. However, the number of samples with a low CEC was small, so further work is necessary to substantiate this conclusion.

ACKNOWLEDGMENTS

The authors thank Nadine Gill for help in the laboratory, Harro Meijer for a working example of the memory correction algorithm, Maria Hoerhold for providing deuterium-depleted water (AWI-TD1), and Stefan Dultz for providing the vermiculite. They thank all providers of soil samples: Lars Kutzbach and Christian Knoblauch (RU-PS2), Christian Siewert (RU-17 and RU-S20), Suzanne Robin Jacobs and Sadadi Ojoatre (KE-20, KE-38, and KE-44), Tobias Wirsing (DE-KA1), and Andre Velescu and Tobias Fabian (EC-BOM and EC-SF1). This work was funded by the Deutsche Forschungsgemeinschaft (DFG, Wi1601/25-1). Open Access funding enabled and organized by Projekt DEAL.

DATA AVAILABILITY STATEMENT

The data can be requested from the authors.

ORCID

Wolfgang Wilcke https://orcid.org/0000-0002-6031-4613

REFERENCES

1. West JB, Bowen GJ, Dawson TE, Tu KP (Eds). *Isoscapes*. Netherlands: Springer; 2010. doi:10.1007/978-90-481-3354-3
2. Bauer KK, Vennemann TW. Analytical methods for the measurement of hydrogen isotope composition and water content in clay minerals by TC/EA. *Chem Geol*. 2014;363:229-240. doi:10.1016/j.chemgeo.2013.10.039
3. Gilg HA, Girard JP, Sheppard SMF. Conventional and Less Conventional Techniques for Hydrogen and Oxygen Isotope Analysis of Clays, Associated Minerals and Pore Waters in Sediments and Soils. In: *Handbook of Stable Isotope Analytical Techniques*. Vol.1. Elsevier; 2004:38-61. doi:10.1016/B978-044451114-0/50004-1
4. Kanik NJ, Longstaffe FJ, Kuligiewicz A, Derkowski A. Systematics of smectite hydrogen-isotope composition: Structural hydrogen versus adsorbed water. *Appl Clay Sci*. 2022;216:106338. doi:10.1016/j.clay.2021.106338
5. VanDeVelde JH, Bowen GJ. Effects of chemical pretreatments on the hydrogen isotope composition of 2:1 clay minerals: Clay mineral isotope treatment effects. *Rapid Commun Mass Spectrom*. 2013;27(10):1143-1148. doi:10.1002/rcm.6554
6. Schimmelmann A. Determination of the concentration and stable isotopic composition of nonexchangeable hydrogen in organic matter. *Anal Chem*. 1991;63(21):2456-2459. doi:10.1021/ac00021a013
7. Hobson KA, Atwell L, Wassenaar LI. Influence of drinking water and diet on the stable-hydrogen isotope ratios of animal tissues. *Proc Natl Acad Sci*. 1999;96(14):8003-8006. doi:10.1073/pnas.96.14.8003
8. Ruppenthal M, Oelmann Y, Wilcke W. Isotope ratios of nonexchangeable hydrogen in soils from different climate zones. *Geoderma*. 2010;155(3-4):231-241. doi:10.1016/j.geoderma.2009.12.005
9. Ruppenthal M, Oelmann Y, Wilcke W. Optimized demineralization technique for the measurement of stable isotope ratios of nonexchangeable H in soil organic matter. *Environ Sci Technol*. 2013;47(2):949-957. doi:10.1021/es303448g
10. Ruppenthal M, Oelmann Y, del Valle HF, Wilcke W. Stable isotope ratios of nonexchangeable hydrogen in organic matter of soils and

plants along a 2100-km climosequence in Argentina: New insights into soil organic matter sources and transformations? *Geochim Cosmochim Acta*. 2015;152:54-71. doi:10.1016/j.gca.2014.12.024
11. Sauer PE, Schimmelmann A, Sessions AL, Topalov K. Simplified batch equilibration for D/H determination of non-exchangeable hydrogen in solid organic material. *Rapid Commun Mass Spectrom*. 2009;23(7):949-956. doi:10.1002/rcm.3954
12. Soto DX, Koehler G, Wassenaar LI, Hobson KA. Re-evaluation of the hydrogen stable isotopic composition of keratin calibration standards for wildlife and forensic science applications. *Rapid Commun Mass Spectrom*. 2017;31(14):1193-1203. doi:10.1002/rcm.7893
13. Wassenaar LI, Hobson KA. Improved method for determining the stable-hydrogen isotopic composition (δD) of complex organic materials of environmental interest. *Environ Sci Technol*. 2000;34(11):2354-2360. doi:10.1021/es990804i
14. Wassenaar LI, Hobson KA. Comparative equilibration and online technique for determination of non-exchangeable hydrogen of keratins for use in animal migration studies. *Isotopes Environ Health Stud*. 2003;39(3):211-217. doi:10.1080/1025601031000096781
15. Schimmelmann A, Lewan MD, Wintsch RP. D/H isotope ratios of kerogen, bitumen, oil, and water in hydrous pyrolysis of source rocks containing kerogen types I, II, IIS, and III. *Geochim Cosmochim Acta*. 1999;63(22):3751-3766. doi:10.1016/S0016-7037(99)00221-5
16. Filot MS, Leuenberger M, Pazdur A, Boettger T. Rapid online equilibration method to determine the D/H ratios of non-exchangeable hydrogen in cellulose. *Rapid Commun Mass Spectrom*. 2006;20(22):3337-3344. doi:10.1002/rcm.2743
17. Chesson LA, Podlesak DW, Cerling TE, Ehleringer JR. Evaluating uncertainty in the calculation of non-exchangeable hydrogen fractions within organic materials. *Rapid Commun Mass Spectrom*. 2009;23(9):1275-1280. doi:10.1002/rcm.4000
18. Grinsted MJ, Wilson AT. Hydrogen isotopic chemistry of cellulose and other organic material of geochemical interest. *N Z J Sci*. 1979;22(3):281-287.
19. Feng X, Krishnamurthy RV, Epstein S. Determination of D/H ratios of nonexchangeable hydrogen in cellulose: A method based on the cellulose-water exchange reaction. *Geochim Cosmochim Acta*. 1993;57(17):4249-4256. doi:10.1016/0016-7037(93)90320-V
20. Bowen GJ, Chesson L, Nielson K, Cerling TE, Ehleringer JR. Treatment methods for the determination of δ^2H and $\delta^{18}O$ of hair keratin by continuous-flow isotope-ratio mass spectrometry. *Rapid Commun Mass Spectrom*. 2005;19(17):2371-2378. doi:10.1002/rcm.2069
21. Qi H, Coplen TB. Investigation of preparation techniques for δ^2H analysis of keratin materials and a proposed analytical protocol. *Rapid Commun Mass Spectrom*. 2011;25(15):2209-2222. doi:10.1002/rcm.5095
22. Hsieh JC, Yapp CJ. Hydrogen-isotope exchange in halloysite: Insight from room-temperature experiments. *Clays Clay Miner*. 1999;47(6):811-816. doi:10.1346/CCMN.1999.0470617
23. Merseburger S, Kessler A, Oelmann Y, Wilcke W. Non-exchangeable stable hydrogen isotope ratios in clay minerals and soil clay fractions: A method test. *Eur J Soil Sci*. 2022;73(4):e13289. doi:10.1111/ejss.13289
24. Merseburger S, Kessler A, Ojoatre S, Berthold C, Oelmann Y, Wilcke W. Global distribution of nonexchangeable stable hydrogen isotope ratios of topsoil clay fractions. *Geochim Cosmochim Acta*. 2023;347:72-87. doi:10.1016/j.gca.2023.02.007
25. Kessler A, Merseburger S, Kappler A, Wilcke W, Oelmann Y. Incorporation of ambient water-H into the C-bonded H Pool of bacteria during substrate-specific metabolism. *ACS Earth Space Chem*. 2022;6(9):2180-2189. doi:10.1021/acsearthspacechem.2c00085
26. Sessions AL, Hayes JM. Calculation of hydrogen isotopic fractionations in biogeochemical systems. *Geochim Cosmochim Acta*. 2005;69(3):593-597. doi:10.1016/j.gca.2004.08.005
27. Ruppenthal M. Stable Isotope Ratios of Nonexchangeable Hydrogen in Bulk Organic Matter as Novel Biogeochemical Tracer. PhD Thesis. University of Tübingen; 2014.
28. Savin SM, Epstein S. The oxygen and hydrogen isotope geochemistry of clay minerals. *Geochim Cosmochim Acta*. 1970;34(1):25-42. doi:10.1016/0016-7037(70)90149-3
29. Ito A, Wagai R. Global distribution of clay-size minerals on land surface for biogeochemical and climatological studies. *Sci Data*. 2017;4(1):170103. doi:10.1038/sdata.2017.103
30. Journet E, Balkanski Y, Harrison S. A new data set of soil mineralogy for dust-cycle modeling. *Atmospheric Chem Phys Discuss*. 2013;13. doi:10.5194/acpd-13-23943-2013
31. FAO. Harmonized World Soil Database: Topsoil CEC (clay), Version 1.1. Published online 2009. Accessed January 31, 2022. https://data.apps.fao.org/map/catalog/srv/eng/catalog.search#/metadata/2427214a-42dc-4862-b58a-00b73cbc7a6f
32. Velde B, Meunier A. *The Origin of Clay Minerals in Soils and Weathered Rocks*. Berlin Heidelberg: Springer; 2008. doi:10.1007/978-3-540-75634-7
33. Hyeong K, Capuano RM. Hydrogen isotope fractionation factor for mixed-layer illite/smectite at 60° to 150°C: New data from the Northeast Texas Gulf Coast 1. *Geochim Cosmochim Acta*. 2004;68(7):1529-1543. doi:10.1016/j.gca.2003.10.002
34. Marumo K, Nagasawa K, Kuroda Y. Mineralogy and hydrogen isotope geochemistry of clay minerals in the Ohnuma geothermal area, northeastern Japan. *Earth Planet Sci Lett*. 1980;47(2):255-262. doi:10.1016/0012-821X(80)90041-2
35. Sheppard SMF, Gilg HA. Stable isotope geochemistry of clay minerals. *Clay Miner*. 1996;31(1):1-24. doi:10.1180/claymin.1996.031.1.01
36. Cornell RM, Schwertmann U. *The Iron Oxides: Structure, Properties, Reactions, Occurrences, and Uses*2nd, completely rev. and extended ed. Wiley-VCH; 2003. doi:10.1002/3527602097
37. Marumo K, Longstaffe FJ, Matsubaya O. Stable isotope geochemistry of clay minerals from fossil and active hydrothermal systems, southwestern Hokkaido, Japan. *Geochim Cosmochim Acta*. 1995;59(12):2545-2559. doi:10.1016/0016-7037(95)00149-2
38. Liu KK, Epstein S. The hydrogen isotope fractionation between kaolinite and water. *Chem Geol*. 1984;46(4):335-350. doi:10.1016/0009-2541(84)90176-1
39. Lawrence JR. O^{18}/O^{16} and D/H Ratios of Soils, Weathering Zones and Clay Deposits. PhD Thesis. California Institute of Technology; 1970. Accessed August 1, 2019. http://resolver.caltech.edu/CaltechETD:etd-01132004-094857
40. Gilg HA, Sheppard SMF. Hydrogen isotope fractionation between kaolinite and water revisited. *Geochim Cosmochim Acta*. 1996;60(3):529-533. doi:10.1016/0016-7037(95)00417-3
41. Méheut M, Lazzeri M, Balan E, Mauri F. First-principles calculation of H/D isotopic fractionation between hydrous minerals and water. *Geochim Cosmochim Acta*. 2010;74(14):3874-3882. doi:10.1016/j.gca.2010.04.020
42. Dogan M, Dogan AU, Yesilyurt FI, Alaygut D, Buckner I, Wurster DE. Baseline studies of the clay minerals society special clays: Specific surface area by the Brunauer Emmett teller (BET) method. *Clays Clay Miner*. 2007;55(5):534-541. doi:10.1346/CCMN.2007.0550508
43. Dogan AU, Dogan M, Onal M, Sarikaya Y, Aburub A, Wurster DE. Baseline studies of the clay minerals society source clays: Specific surface area by the Brunauer Emmett teller (BET) method. *Clays Clay Miner*. 2006;54(1):62-66. doi:10.1346/CCMN.2006.0540108
44. Mermut AR, Angel CF. Baseline studies of the clay minerals society source clays: Chemical analyses of major elements. *Clays Clay Miner*. Published online. 2001;49(5):381-386. doi:10.1346/CCMN.2001.0490504

45. Guggenheim S, Van Groos AK. Baseline studies of the clay minerals society source clays: Thermal analysis. *Clays Clay Miner*. 2001;49(5):433-443. doi:10.1346/CCMN.2001.0490509
46. Kogel JE, Lewis SA. Baseline studies of the clay minerals society source clays: Chemical analysis by inductively coupled plasma-mass spectroscopy (ICP-MS). *Clays Clay Miner*. 2001;49(5):387-392. doi:10.1346/CCMN.2001.0490505
47. Chipera SJ, Bish DL. Baseline studies of the clay minerals society source clays: Powder X-ray diffraction analyses. *Clays Clay Miner*. 2001;49(5):398-409. doi:10.1346/CCMN.2001.0490507
48. Borden D, Giese RF. Baseline studies of the clay minerals society source clays: Cation exchange capacity measurements by the ammonia-electrode method. *Clays Clay Miner*. 2001;49(5):444-445. doi:10.1346/CCMN.2001.0490510
49. Hower J, Mowatt TC. The mineralogy of illites and mixed-layer illite/montmorillonites. *Am Mineral*. 1966;51(5-6):825-854. doi:10.1346/CCMN.1999.0470617
50. Dultz S, Riebe B, Bunnenberg C. Temperature effects on iodine adsorption on organo-clay minerals: II. Structural effects. *Appl Clay Sci*. 2005;28(1):17-30. doi:10.1016/j.clay.2004.01.005
51. Bors J, Gorny A, Dultz S. Iodide, caesium and strontium adsorption by organophilic vermiculite. *Clay Miner*. 1997;32(1):21-28. doi:10.1180/claymin.1997.032.1.04
52. Steudel A, Weidler PG, Schuhmann R, Emmerich K. Cation exchange reactions of vermiculite with cu-triethylenetetramine as affected by mechanical and chemical pretreatment. *Clays Clay Miner*. 2009;57(4):486-493. doi:10.1346/CCMN.2009.0570409
53. Steudel A. Selection Strategy and Modification of Layer Silicates for Technical Applications. Univ.-Verlag Karlsruhe; 2008. Accessed March 6, 2017. doi:10.5445/IR/1000010008
54. Qi H, Coplen TB, Gehre M, et al. New biotite and muscovite isotopic reference materials, USGS57 and USGS58, for δ^2H measurements–a replacement for NBS 30. *Chem Geol*. 2017;467:89-99. doi:10.1016/j.chemgeo.2017.07.027
55. Fabian T, Velescu A, Wilcke W. Soil development on heterogeneous parent material under tropical montane forest in South Ecuador. *Tabebuia Bull*. 2019;6:7. doi:10.5678/lcrs/pak823-825.cit.1399
56. Fabian T, Velescu A, Harteif K, Wilcke W. Soil properties of the cloud forest in Cajanuma and of the pastures along an elevation gradient from 1000 to 3000 m a.s.l. *Tabebuia Bull*. 2020;7:9. doi:10.5678/LCRS/FOR2730.CIT.1817
57. Schrumpf M, Guggenberger G, Valarezo C, Zech W. Tropical montane rain forest soils: Development and nutrient status along an altitudinal gradient in the south Ecuadorian Andes. *Erde*. 2001;132(1):43-59.
58. Wilcke W, Yasin S, Abramowski U, Valarezo C, Zech W. Nutrient storage and turnover in organic layers under tropical montane rain forest in Ecuador. *Eur J Soil Sci*. 2002;53(1):15-27. doi:10.1046/j.1365-2389.2002.00411.x
59. Ojoatre S. Deforestation and Recovery of the Tropical Montane Forests of East Africa. PhD Thesis. Lancaster University; 2022. Accessed May 18, 2022. http://www.research.lancs.ac.uk/portal/services/downloadRegister/356576715/2021OjoatrePhD.pdf
60. Messmer ST, Elsenbeer H, Wilcke W. High exchangeable calcium concentrations in soils on Barro Colorado Island, Panama. *Geoderma*. 2014;217-218:212-224. doi:10.1016/j.geoderma.2013.10.021
61. Messmer ST. Biotic and Abiotic Drivers of the Base Metal Cycling in a Tropical Lowland Rain Forest in Panama. PhD Thesis. University of Bern; 2014.
62. Siewert C. Investigation of the thermal and biological stability of soil organic matter. Shaker; 2001.
63. Siewert C. Rapid screening of soil properties using Thermogravimetry. *Soil Sci Soc Am J*. 2004;68(5):1656-1661. doi:10.2136/sssaj2004.1656
64. Knoblauch C, Beer C, Schuett A, et al. Carbon dioxide and methane release following abrupt thaw of pleistocene permafrost deposits in Arctic Siberia. *J Geophys Res Biogeo*. 2021;126(11):e2021JG006543. doi:10.1029/2021JG006543
65. Lobe I. Untersuchungen zur Schwermetallbelastung von Böden der Nord-Slowakei. Diploma thesis. University of Bayreuth; 1997.
66. Lobe I, Wilcke W, Kobža J, Zech W. Heavy metal contamination of soils in northern Slovakia. *Z Pflanzenernähr Bodenkd*. 1998;161(5):541-546. doi:10.1002/jpln.1998.3581610507
67. Bandowe BAM, Shukurov N, Kersten M, Wilcke W. Polycyclic aromatic hydrocarbons (PAHs) and their oxygen-containing derivatives (OPAHs) in soils from the Angren industrial area, Uzbekistan. *Environ Pollut*. 2010;158(9):2888-2899. doi:10.1016/j.envpol.2010.06.012
68. Shukurov N, Pen-Mouratov S, Steinberger Y, Kersten M. Soil biogeochemical properties of Angren industrial area, Uzbekistan. *J Soil Sediment*. 2009;9(3):206-215. doi:10.1007/s11368-009-0079-8
69. Mehra OP, Jackson ML. Iron oxide removal from soils and clays by a dithionite-citrate system buffered with sodium bicarbonate. In: *Proceedings 7th Nat. Conf. Clays*. Vol 5.; 1960:317–327. Accessed July 29, 2014. http://www.cabdirect.org/abstracts/19601901561.html
70. DIN ISO 11277. *Bodenbeschaffenheit - Bestimmung Der Partikelgrößenverteilung in Mineralböden*. Verfahren Mittels Siebung Und Sedimentation. Beuth Verlag; 2002. Accessed March 9, 2017. doi:10.31030/9283499
71. Abbott A. DIY Glove Bag. aprilabbott. Published November 11, 2019. Accessed February 22, 2021. https://aprilabbott.wordpress.com/2019/11/11/diy-glove-bag/
72. Wassenaar LI, Hobson KA, Sisti L. An online temperature-controlled vacuum-equilibration preparation system for the measurement of δ^2H values of non-exchangeable-H and of δ^{18}O values in organic materials by isotope-ratio mass spectrometry. *Rapid Commun Mass Spectrom*. 2015;29(5):397-407. doi:10.1002/rcm.7118
73. Polyakov VB, Horita J, Cole DR. Pressure effects on the reduced partition function ratio for hydrogen isotopes in water. *Geochim Cosmochim Acta*. 2006;70(8):1904-1913. doi:10.1016/j.gca.2006.01.010
74. Horita J, Wesolowski DJ. Liquid-vapor fractionation of oxygen and hydrogen isotopes of water from the freezing to the critical temperature. *Geochim Cosmochim Acta*. 1994;58(16):3425-3437. doi:10.1016/0016-7037(94)90096-5
75. Guidotti S, Jansen HG, Aerts-Bijma AT, Verstappen-Dumoulin BMAA, van Dijk G, Meijer HAJ. Doubly labelled water analysis: Preparation, memory correction, calibration and quality assurance for delta δ^2H and δ^{18}O measurements over four orders of magnitudes. *Rapid Commun Mass Spectrom*. 2013;27(9):1055-1066. doi:10.1002/rcm.6540
76. Ammann L, Bergaya F, Lagaly G. Determination of the cation exchange capacity of clays with copper complexes revisited. *Clay Miner*. 2005;40(4):441-453. doi:10.1180/0009855054040182
77. Meier LP, Kahr G. Determination of the cation exchange capacity (CEC) of clay minerals using the complexes of copper (II) ion with Triethylenetetramine and Tetraethylenepentamine. *Clays Clay Miner*. 1999;47(3):386-388. doi:10.1346/CCMN.1999.0470315
78. Soil Survey Staff. *Keys to Soil Taxonomy*. 12thed. United States Department of Agriculture, Natural Resources Conservation Service; 2014.
79. Bergaya F, Lagaly G, Vayer M. Cation and anion exchange. In: *Developments in Clay Science*. Vol.5. Elsevier; 2013:333-359.
80. Paul D, Skrzypek G, Fórizs I. Normalization of measured stable isotopic compositions to isotope reference scales – A review. *Rapid Commun Mass Spectrom*. 2007;21(18):3006-3014. doi:10.1002/rcm.3185
81. R Core Team. *R: A language and environment for statistical* Comput Secur; 2022. https://www.R-project.org/
82. Wickham H, Averick M, Bryan J, et al. Welcome to the tidyverse. *J Open Source Softw*. 2019;4(43):1686. doi:10.21105/joss.01686

83. Fick SE, Hijmans RJ. WorldClim 2: New 1-km spatial resolution climate surfaces for global land areas. *Int J Climatol*. 2017;37(12):4302-4315. doi:10.1002/joc.5086
84. Trabucco A, Zomer R. Global Aridity Index and Potential Evapotranspiration (ET0) Climate Database v2. Published online 2019:1705236666 Bytes. doi:10.6084/M9.FIGSHARE.7504448.V3
85. Bowen GJ, Revenaugh J. Interpolating the isotopic composition of modern meteoric precipitation: Isotopic composition of modern precipitation. *Water Resour Res*. 2003;39(10):1299-1312. doi:10.1029/2003WR002086
86. Bowen GJ. WaterIsotopes.org. The online isotopes in precipitation calculator, version 3.1. Published 2022. Accessed April 28, 2021. http://wateriso.utah.edu/waterisotopes/pages/data_access/oipc.html
87. Bigeleisen J. Chemistry of isotopes: Isotope chemistry has opened new areas of chemical physics, geochemistry, and molecular biology. *Science*. 1965;147(3657):463-471. doi:10.1126/science.147.3657.463
88. Kosmulski M. The pH dependent surface charging and points of zero charge. IX update. *Adv Colloid Interface Sci*. 2021;296:102519. doi:10.1016/j.cis.2021.102519

SUPPORTING INFORMATION

Additional supporting information can be found online in the Supporting Information section at the end of this article.

How to cite this article: Merseburger S, Kessler A, Oelmann Y, Wilcke W. Equilibrium isotope fractionation factors of H exchange between steam and soil clay fractions. *Rapid Commun Mass Spectrom*. 2023;37(10):e9499. doi:10.1002/rcm.9499